Mineralogical Magazine, June 2012, Vol. 76(3), pp. 707–716

A reinvestigation of mayenite from the type locality, the Ettringer Bellerberg volcano near Mayen, Eifel district, Germany

E. V. Galuskin*, J. Kusz, T. Armbruster, R. Bailau, I. O. Galuskina, B. Ternes and M. Murashko[5]

[1] Faculty of Earth Sciences, Department of Geochemistry, Mineralogy and Petrography, University of Silesia, Będzińska 60, 41-200 Sosnowiec, Poland
[2] Institute of Physics, University of Silesia, Uniwersytecka 4, 40-007 Katowice, Poland
[3] Mineralogical Crystallography, Institute of Geological Sciences, University of Bern, Freiestrasse 3, CH-3012 Bern, Switzerland
[4] Dienstleistungszentrum ländlicher Raum (DLR) Westerwald-Osteifel-Aussenstelle Mayen, Bahnhofstrasse 45, 56727 Mayen, Germany
[5] Systematic Mineralogy, 44, 11th line V.O, apt. 76, Saint Petersburg 199178, Russia

[*Received 28 February 2012; Accepted 19 April 2012; Associate Editor: Edward Grew*]

ABSTRACT

New electron-microprobe analyses of mayenite from the Ettringer Bellerberg volcano near Mayen in the Eifel district, Germany have high Cl contents and Raman spectroscopy indicates the presence of OH groups. Neither of these components is included in the generally accepted chemical formula, $Ca_{12}Al_{14}O_{33}$. A refinement of the crystal structure by single-crystal X-ray methods reveals a previously unrecognized partial substitution. The O2 site which forms one of the apices of an AlO_4 tetrahedron (with $3 \times$ O1 sites) is replaced by $3 \times$ O2a sites, which change the coordination of the central Al atom from tetrahedral to octahedral. This substitution is related to partial hydration of $Ca_{12}Al_{14}O_{32}Cl_2$ according to the isomorphic scheme $(O^{2-} + Cl^{-}) \leftrightarrow 3(OH)^{-}$. The revised composition of Eifel mayenite is best described by the formula $Ca_{12}Al_{14}O_{32-x}Cl_{2-x}(OH)_{3x}$ (x ~0.75); the original formula, $Ca_{12}Al_{14}O_{33}$, is inadequate. The analysed mineral can be considered to consist of endmember $Ca_{12}Al_{14}O_{32}Cl_2$ (62.5 mol.%) and endmember $Ca_{12}Al_{14}O_{30}(OH)_6$ (37.5 mol.%).

Keywords: mayenite, brearleyite, Raman spectroscopy, structure, Ettringer Bellerberg volcano, Mayen, Eifel, Germany.

Introduction

Mayenite, $Ca_{12}Al_{14}O_{33}$, occurs rarely as micrometre-sized crystals in sanidinite facies larnite- and/or spurrite-bearing metasomatic rocks. It was first described from altered xenoliths in volcanic rocks at Bellerberg in the Eifel district, Rhineland-Palatinate, Germany (Hentschel, 1964), and has subsequently been identified in pyrometamorphic rocks of the Mottled Zone in the Hatrurim Formation, Israel (Gross, 1977). Three minerals related to mayenite: wadalite $Ca_{12}Al_{10}Si_4O_{32}Cl_6$, from Koriyama City, Fukushima Prefecture, Japan (Tsukimura *et al*., 1993); brearleyite, $Ca_{12}Al_{14}O_{32}Cl_2$, from a Ca- and Al-rich refractory inclusion in the Northwest Africa 1934 meteorite (Ma *et al*., 2011); and eltyubyite, $Ca_{12}Fe^{3+}_{10}Si_4O_{32}Cl_6$, from the Upper Chegem caldera, Northern Caucasus, Russia (Galuskin *et al*., 2011); have been reported from terrestrial or meteoritic environments. Although it is rare in nature, mayenite and its synthetic

* E-mail: evgeny.galuskin@us.edu.pl
DOI: 10.1180/minmag.2012.076.3.18

analogues are of considerable interest as they have potential applications as transparent conductors, catalysts for the combustion of organic compounds, oxygen ion conductors, ion emitters and luminescent matrices (Hosono *et al*., 2007; Iwata *et al*., 2008; Li *et al*., 2009).

The composition and crystal structure of naturally occurring mayenite are poorly constrained and many interesting questions remain. A reinvestigation of mayenite from the type locality revealed the presence of a significant amount of Cl (Table 1), a chemical constituent which was not reported in the original mineral description, but which has been found in a mayenite-like phase with a formula $Ca_{12}Al_{14}O_{32}Cl_2{\cdot}3H_2O$ in altered xenoliths in ignimbrites from the Upper Chegem caldera, Northern Caucasus, Russia (Galuskin *et al*., 2009), and in the related mineral brearleyite (Ma *et al*., 2011). An investigation of the composition of mayenite from Israel has shown that it contains significant F (up to 1.9 a.p.f.u.; authors' unpublished data). These data show that halogens play an important role in mayenite and related minerals. The low analytical totals (Table 1) also suggest a role for hydroxyl groups or water molecules. To better characterize these roles, mayenite from the Eifel district was investigated by single-crystal X-ray methods and Raman spectroscopy.

The results of our investigation are of interest to a wide scientific community as synthetic $Ca_{12}Al_{14}O_{33}$, for which the name 'mayenite' is used historically, is a nanoporous material (Matsuishi *et al*., 2003; Palacios *et al*., 2007, 2008; Hosono *et al*., 2009; Sakakura *et al*., 2011). Mayenite crystallizes in space group $I\bar{4}3d$ with a = 11.98 Å. Its unusual properties are related to its cage structure, which contains 32 of the 33 oxygen anions in a calcium aluminate framework (Büssem and Eitel, 1936; Bartl and Scheller, 1970; Boysen *et al*., 2007, 2009). The 'free' extraframework oxygen anion is distributed over 1/6 of the large cages in the framework and can diffuse through large openings between adjacent cages (Matsuishi *et al*., 2009; Boysen *et al*., 2010; Janak and Lee, 2010). The true mayenite structure is heavily disordered due to displacements of

TABLE 1. Composition of mayenite from Eifel, Germany.

Oxide	Mean†	Standard deviation	Range
TiO_2	0.02	0.02	0–0.08
SiO_2	0.03	0.02	0–0.05
Al_2O_3	46.38	0.34	45.46–46.99
Fe_2O_3	2.50	0.10	2.32–2.64
CaO	45.31	0.33	44.66–46.02
MgO	0.03	0.02	0–0.05
Cl	3.16	0.16	2.81–3.38
−O=Cl	−0.71		
Total	96.72		
H_2O	1.23		
Total (incl. H_2O)	97.95		
Formula based on 26 cations			
Ca/X	12.000		
Al	13.513		
Mg	0.012		
Si	0.007		
Ti^{4+}	0.003		
Fe^{3+}	0.465		
Y	14.000		
Cl	1.323		
OH*	2.028		

† The mean is calculated for n = 12.

* Calculated as 3(2 − Cl) p.f.u. on the basis of the general formula $Ca_{12}Al_{14}O_{32-x}Cl_{2-x}(OH)_{3x}$.

cations and anions associated with the 'free' oxygen in the cages (Sakakura *et al*., 2011). Other extraframework anions can substitute for the 'free' oxygen in the mayenite structure, producing anionic conductors. A family of compounds with the composition $Ca_{12}Al_{14}O_{32}W$, where $W = O^{2-}$, $2O^{-}$, $2F^{-}$, $2Cl^{-}$, $2OH^{-}$, S^{2-}, $2e^{-}$, $2H^{-}$, N_2^{2-}, SO_4^{2-} and others, have been described (Iwata *et al*., 2008; Hayashi, 2011).

Experimental

Single-crystal X-ray studies of mayenite from the Eifel district were carried out using a SuperNova Dual diffractometer with a mirror monochromator (Mo$K\alpha$, $\lambda = 0.71073$ Å) and Atlas CCD detector (Aligent Technologies) at the Institute of Physics, University of Silesia. Experimental details are summarized in Table 2. The structure was solved by direct methods, with subsequent analyses of difference-Fourier maps, and refined with neutral atom scattering factors using *SHELX97* (Sheldrick, 2008).

Raman spectra of single crystals of mayenite were obtained using a Dilor XY Raman spectrometer (Bayerisches Geoinstitute, University of Bayreuth, Germany), equipped with a 1800 line mm^{-1} grating monochromator and a charge-coupled device Peltier-cooled detector, on an Olympus BX40 confocal microscope. The incident excitation was provided by a water-cooled argon laser operating at 514.5 nm. The power at the exit of a 100× objective lens varied from 30 to 50 mW. Raman spectra were recorded in backscattered geometry in the range 100–4000 cm^{-1} with a resolution of 2 cm^{-1}. Collection times of 20 s and accumulations of five scans were used. The monochromator was calibrated using the Raman scattering line of a silicon plate (520.7 cm^{-1}).

The morphology and composition were investigated using a Philips XL30/EDAX scanning electron microscope (Department of Earth Sciences, University of Silesia, Poland) and a CAMECA SX100 electron microprobe operating in wavelength-dispersive spectrometry mode at

TABLE 2. Data collection and structure refinement details for Eifel mayenite.

Cell dimensions (Å)	$a = 12.0320(4)$
Cell volume (Å^3)	1741.86(1)
Space group	$I\bar{4}3d$
Z	2
Radiation (wavelength, Å)	Mo$K\alpha$ (0.71073)
Temperature (K)	100
Crystal size (mm)	$0.097 \times 0.131 \times 0.172$
Time per frame (s)	60
Number of frames	742
Completeness	0.997
Average redundancy	45.8
Reflections collected	59,329
Maximum θ	45.64
Index range	$-24 \leqslant h \leqslant 22$
	$-24 \leqslant k \leqslant 24$
	$-22 \leqslant l \leqslant 24$
Unique reflections	1244
Reflections $I > 4\sigma(I)$	1243
Number of parameters	37
R_{int}	0.0347
R_σ	0.0074
GooF	1.169
R_1, $I > 4\sigma(I)$	0.0117
R_1, all data	0.0117
wR_2 (on F^2)	0.0346
$\Delta\rho_{min}$ (e$^-$ Å^{-3})	−0.46 close to Ca
$\Delta\rho_{max}$ (e$^-$ Å^{-3})	0.78 close to Ca

TABLE 3. Atom coordinates, equivalent isotropic displacement parameters (Å^2), and occupancies for Eifel mayenite.

Site	*x*/*a*	*y*/*b*	*z*/*c*	U_{eq}	Occupancy	a.p.f.u.
Ca	0.137841(11)	0.0	0.25	0.00593(3)	1	12
Al1	0.016173(13)	0.016173(13)	0.016173(13)	0.00464(7)	0.943(2)	7.54(2) Al + 0.46 Fe
Al2	0.875	0.0	0.25	0.00326(5)	1	6
O1	0.03539(3)	0.44472(3)	0.15013(3)	0.00681(6)	1	24
O2	0.18393(4)	0.18393(4)	0.18393(4)	0.00778(12)	0.905(2)	7.24(2)
O2a	0.2010(4)	0.2849(3)	0.1055(4)	0.0074(8)	0.094(2)	2.26(5)
Cl	0.375	0.0	0.25	0.00920(16)	0.208	1.25

15 kV, 10−20 nA with a 1−3 μm beam diameter (Institute of Geochemistry, Mineralogy and Petrology, University of Warsaw, Poland). The following lines and standards were used for quantitative analyses: Ca*K*α, Si*K*α, wollastonite; Fe*K*α, hematite; Ti*K*α, rutile; Mn*K*α, rhodochrosite; Mg*K*α, diopside; Na*K*α, albite; Al*K*α, orthoclase; S*K*α, baryte; F*K*α, fluorphlogopite; and Cl*K*α, tugtupite.

Crystal structure of mayenite from the Eifel district

The general crystal-chemical formula of mayenite–wadalite can be written $X_{12}T1_8T2_6O1_{24}O2_8W_6$, where *X* is a Ca site with sevenfold coordination, *T*1 is a trigonal pyramid centred on Al or on cations such as Fe^{3+}, Mg or Ti, and *T*2 is an ideal Al tetrahedron, which is also the preferred position for Si. The *W* site is in the centre of a large cage (~5 Å in diameter) which is only partially filled in mayenite, $Ca_{12}Al_8Al_6O_{24}O_8(O_1\square_5)$, and brearleyite, $Ca_{12}Al_8Al_6O_{24}O_8(Cl_2\square_4)$. The number of additional anions in the structural cages (Cl^- in the following example) increases as Si replaces Al in the framework according to the scheme $Si^{4+} + Cl^- \leftrightarrow Al^{3+} + \square$ leading to full cages in wadalite $Ca_{12}Al_8(Al_2Si_4)O_{24}O_8Cl_6$ (Tsukimura *et al*., 1993; Mihajlović *et al*., 2004).

Single-crystal X-ray data for mayenite from the Eifel district were collected at 100 K to reduce contributions from thermal disorder and obtain a high positional resolution. Refinement results obtained in space group $I\bar{4}3d$ [a = 12.0320(4) Å, V = 1741.86(1) Å^3] (Tables 2−5) are similar to those for synthetic mayenite and its structural derivatives (Bartl and Scheller, 1970; Boysen *et al*., 2007; Palacios *et al*., 2007; Iwata *et al*., 2008; Sakakura *et al*., 2011); but there are some significant differences. In spite of the acentric space group $I\bar{4}3d$, the investigated crystal did not show any indication of twinning as the Flack parameter converged to −0.02(2). The structure solution completed by difference-Fourier analyses indicated threefold positional disorder around O2. Satellite densities (designated as O2a) were observed 1.55 Å from O2 (Fig. 1). These satellites

TABLE 4. Anisotropic displacement parameters (Å^2) for Eifel mayenite.

Site	U_{11}	U_{22}	U_{33}	U_{23}	U_{13}	U_{12}
Ca	0.00688(5)	0.00654(5)	0.00436(4)	0.00055(4)	0.000	0.000
Al1	0.00464(7)	0.00464(7)	0.00464(7)	0.00103(4)	0.00103(4)	0.00103(4)
Fe1	0.00464(7)	0.00464(7)	0.00464(7)	0.00103(4)	0.00103(4)	0.00103(4)
Al2	0.00273(9)	0.00353(6)	0.00353(6)	0	0	0
O1	0.00775(12)	0.00608(12)	0.00660(13)	0.00075(9)	−0.00347(10)	−0.00173(9)
O2	0.00778(12)	0.00778(12)	0.00778(12)	−0.00180(11)	−0.00180(11)	−0.00180(11)
O2a	0.0090(15)	0.0023(12)	0.0108(15)	−0.0023(10)	0.0002(11)	0.0012(10)
Cl	0.0036(3)	0.0120(3)	0.0120(3)	0	0	0

TABLE 5. Selected bond lengths (Å) for Eifel mayenite.

Ca	−O1	2.3859(4) ×2
	−O1	2.4961(4) ×2
	−O2	2.4160(4) ×2
	−Cl3	2.8535(2)
	−O2a	2.256(4) ×2
	−O2a	2.485(5) ×2
Al1	−O1	1.7900(4) ×3
	−O2	1.7140(8)
	−O2a	2.0984(5) ×3
Al2	−O1	1.7461(4) ×4
O2a	−Cl	1.770(5)
O2a	−O2	1.552(4)

form a triangle around O2 with an O2a−O2a separation of ~2.66 Å. The short distance between the O2 and O2a sites means that they both cannot be occupied simultaneously. Thus vacancies at O2 were assumed in the refinement, which was constrained to a previously confirmed O2 vacancies to O2a population ratio of 1/3. The partial substitution of O2 (~10%) by 3 × O2a is reported for the first time (Table 3). The O2 and 3 × O1 oxygen atoms form the apices of the *T*1 (AlO_4) tetrahedron (Fig. 2*a*). If O2 is replaced by 3 × O2a the coordination of the central Al atom changes from tetrahedral to octahedral (Fig. 2*b*). This change in coordination results in a small shift in the Al at the *T*1 site towards the centre of the O2a triangle, which is evident in the increased and anisotropic displacement parameter of *T*1 (Fig. 1; Table 4). As there are two bonds between O2a and Ca and one bond between O2a and octahedral *T*1, bond-strength arguments indicate that an OH group occupies the O2a site.

Initial test refinements indicated that Fe is concentrated at *T*1 and that *T*2 is occupied by Al. Subsequent refinements allowed the Fe and Al occupancy at *T*1 to be varied. The high crystal quality (low mosaicity) required an extinction correction. To exclude the observed high correlations between Cl occupancy and Cl atom displacement parameters, the Cl occupancy was fixed at the stoichiometric value of 0.208.

Although only 10% of *T*1 has an octahedral coordination, we performed test refinements with split *T*1 positions (with fixed occupancies of 0.9 and 0.1, respectively). For octahedral *T*1 the *T*−O distances were restrained to 1.94(1) Å. In subsequent refinements Al1(oct) converged at 0.0045(1), 0.0045(1), 0.0045(1) with

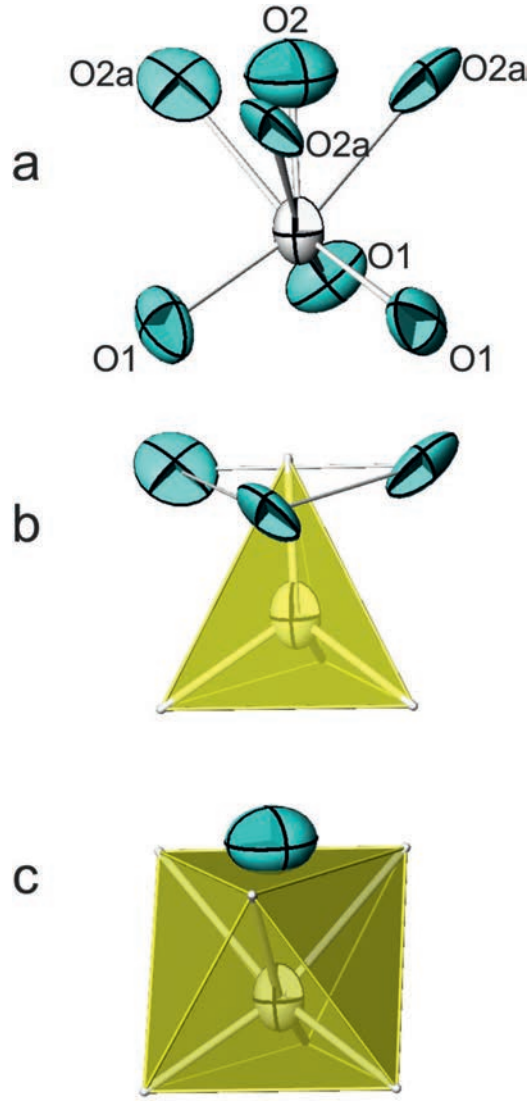

FIG. 1. Coordination of the *T*1 site in Eifel mayenite. (*a*) A threefold axis passes through O2 and *T*1 (white). The occupancy of O2a is ~10% and there are ~10% vacancies at O2. For clarity (using data obtained at 100 K) the displacement ellipsoids corresponding to 99.99% probability are enlarged by a factor of three. (*b*) If O2a sites are vacant *T*1 has tetrahedral coordination and is surrounded by O2 and 3 × O1. Displacement ellipsoids of O2a are connected by lines to emphasize their triangular arrangement. (*c*) If O2 is vacant the *T*1 site adopts an octahedral coordination in which the central atom is surrounded by 3 × O1 and 3 × O2a. The displacement ellipsoid for *T*1 is slightly elongated along the threefold axis due to a statistical overlay of the octahedral and tetrahedral coordination.

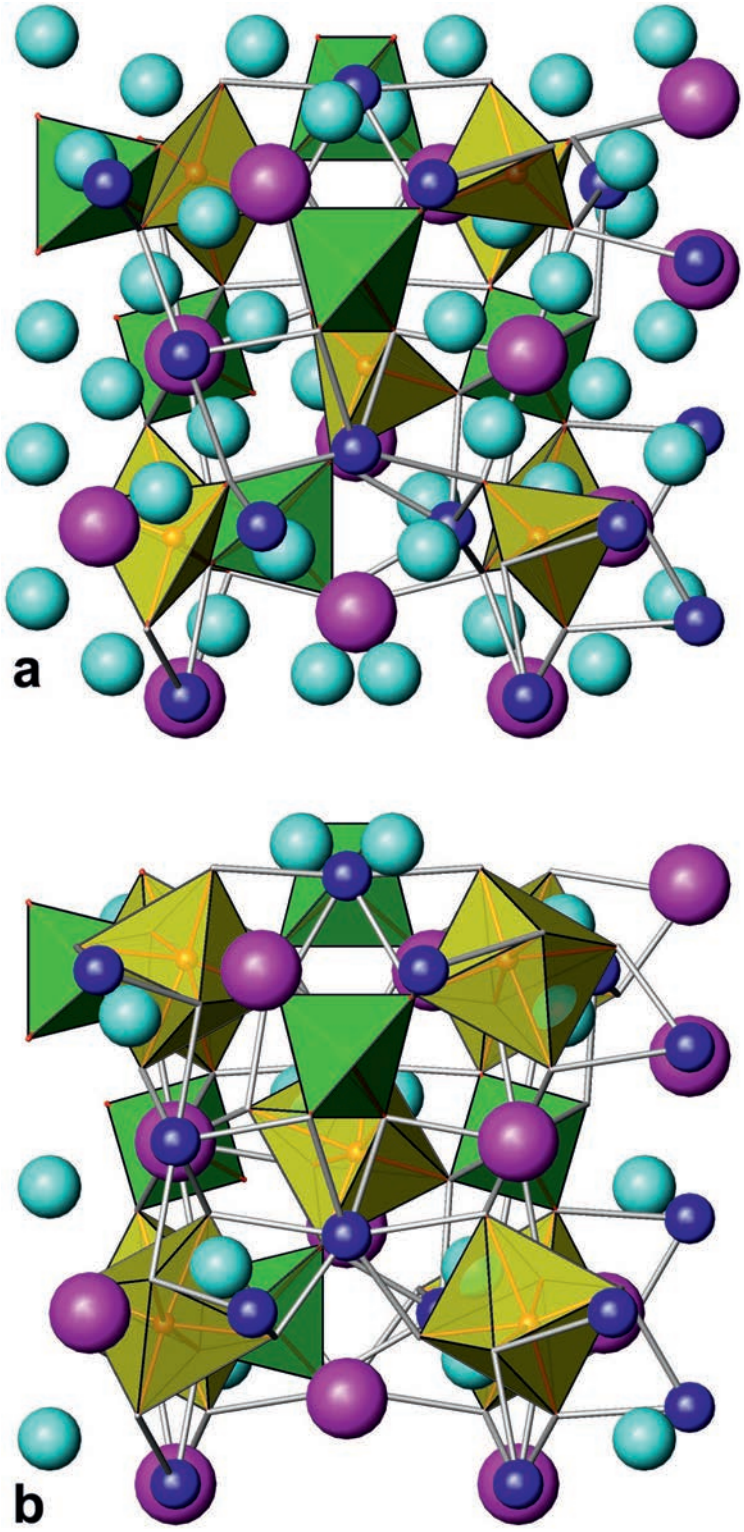
a
b

Al1(oct)–O1 1.917(1) Å and Al1(oct)–O2a 1.940(1) Å, respectively. The distance between Al1(oct) and Al1(tet) is 0.26 Å. In addition, the displacement parameters of Al1(tet) gave an essentially spherical shape.

There are three configurations of coordination and occupancies in mayenite, which are apportioned as follows: (1) 22% of cages have Cl at *W*, which is located linearly between two Ca ions at a distance of 2.85 Å (Table 5) with cage walls formed by four *T*1-tetrahedra and four *T*2-tetrahedra; (2) 37% of cages have one octahedron at *T*1 produced by the substitution O2 → (3 × O2a) with the remaining *T*1 and *T*2 sites in tetrahedral coordination; and (3) 41% of cages are empty and are associated with *T*1 and *T*2 tetrahedra. The crystal-chemical formula calculated on the basis of the structural data is $Ca_{12}(Al_{7.54}Fe^{3+}_{0.46})_{\Sigma 8}Al_6(O_{24}O_{7.24}\square_{0.76})_{\Sigma 32}[Cl_{1.25}(OH)_{2.26}\square_{2.49}]_{\Sigma 6}$, which is close to the formula $Ca_{12}(Al_{13.513}Fe^{3+}_{0.465}Mg_{0.012}Si_{0.007}Ti^{4+}_{0.003})_{\Sigma 14}(O_{31.323}\square_{0.677})_{\Sigma 32}[Cl_{1.323}(OH)_{2.028}\square_{2.649}]_{\Sigma 6}$ obtained from electron-probe microanalysis (Table 1).

Raman spectroscopy

The main bands in the Raman spectrum of Eifel mayenite (Fig. 3) are at 881, 772, 703, 512 and 323 cm^{-1}. These bands correspond to those of synthetic mayenite $Ca_{12}Al_{14}O_{33}$ (Tolkacheva *et al*., 2011) and $Ca_{12}Al_{14}O_{32}Cl_2$ (Sun *et al*., 2009) and are assigned as follows: 880 and 770 cm^{-1} are stretching vibrations of Al–O in $[AlO_4]^{5-}$ (asymmetric and symmetric, respectively); 510 cm^{-1} is a bending vibrations of Al–O in $[AlO_4]^{5-}$; 330 cm^{-1} is due to vibrations of Ca[AlO_4] and Ca–O. An additional band near 700 cm^{-1} is assigned to the symmetric stretching vibrations of $[Fe^{3+}O_4]^{5-}$. Bands at about 890 and 1100 cm^{-1}, which would indicate the presence of O_2^- and O_2^{2-} ions, respectively, are absent in mayenite spectra (Palacios *et al*., 2007; Ruszak *et al*., 2007; Li *et al*., 2009).

Bands at 3669, 3644 and 3598 cm^{-1} (OH vibrations) and a broad weak band centred at about 3400 cm^{-1} (which might be due to H_2O) are observed in the O–H stretching region (Fig. 3). The band near 3575 cm^{-1} that is characteristic of synthetic mayenite (Ruszak *et al*., 2007) is very small in our spectra; this band is related to the hydration of mayenite by the reaction $Ca_{12}Al_{14}O_{33} + H_2O \rightarrow Ca_{12}Al_{14}O_{32}(OH)_2$.

In summary, the Raman spectra provide evidence that the deficit in the totals of the electron-probe microanalyses of mayenite (Table 1) can be attributed to the presence of water or hydroxyl in its structure, at least in part.

Discussion

The structure of $Ca_{12}Al_{14}O_{33}$ (which can be written $12CaO{\cdot}7Al_2O_3$ or $C_{12}A_7$ in cement chemists' notation) was first determined by Büssem and Eitel (1936). There are structure solutions for synthetic mayenite-like phases with the compositions $Ca_{12}Al_{14}O_{33}$ ($I\bar{4}3d$, $a \sim 11.99$ Å; Bartl and Scheller, 1970; Boysen *et al*., 2007; Palacios *et al*., 2007; Sakakura *et al*., 2011); $Ca_{12}Al_{14}O_{32}F_2$ ($I\bar{4}3d$, $a \sim 11.98$ Å; Williams, 1973; Qijun *et al*., 1997); $Ca_{12}Al_{14}O_{32}Cl_2$ ($I\bar{4}3d$, $a \sim 12.01$ Å; Iwata *et al*., 2008); and $Ca_{12}Al_{10.6}Si_{3.4}O_{32}Cl_{5.4}$, a wadalite-like phase ($I\bar{4}3d$, $a \sim 11.98$ Å; Feng *et al*., 1988; Fujita *et al*., 2001). Furthermore, the structure of wadalite from the type locality in Fukushima, Japan $(Ca_{11.76}Mg_{0.46})[(Al_{8.52}Fe_{0.92})Si_4O_{31.36}]Cl_{5.28}$ ($I\bar{4}3d$, $a \sim 12.03$ Å; Tsukimura *et al*., 1993) and from the Eifel district, Germany $Ca_{12.00}[(Si_{3.88}Al_{2.65}Fe_{1.32}Ti_{0.15})(Al_{4.73}Mg_{0.68}Si_{0.30}Fe_{0.29})O_{32}]Cl_{5.69}$ ($I\bar{4}3d$, $a \sim 12.03$ Å; Mihajlović *et al*., 2004) has also been reported. A single-crystal synchrotron diffraction study of synthetic $Ca_{12}Al_{14}O_{33}$ [$I\bar{4}3d$, $a = 11.989(3)$] showed that the incorporation of O^{2-} ions in one of the six structural cages causes a shift of all the ions surrounding the cages except *T*2, but without changes in the coordination of cations (Sakakura *et al*., 2011).

Structure refinement of Eifel mayenite has revealed a new mechanism for the incorporation of additional ions into the structural cages,

FIG. 2 (*facing page*). (*a*) The original model of mayenite with Al1 (yellow) and Al2 (green) represented as tetrahedra, O2 is at the tetrahedral apex of Al1. The O2a sites are shown as pale blue spheres, Cl as pink spheres and Ca as dark blue spheres. (*b*) In the new model the Al1 site is octahedrally coordinated by 3 × O2a if O2 is vacant. The Al1 site is shifted from the centre, producing irregular Al–O distances. This is probably an artefact as 90% of Al1 is tetrahedral. In comparison to Al2, Al1 has greater anisotropic displacement parameters, in line with the above interpretation.

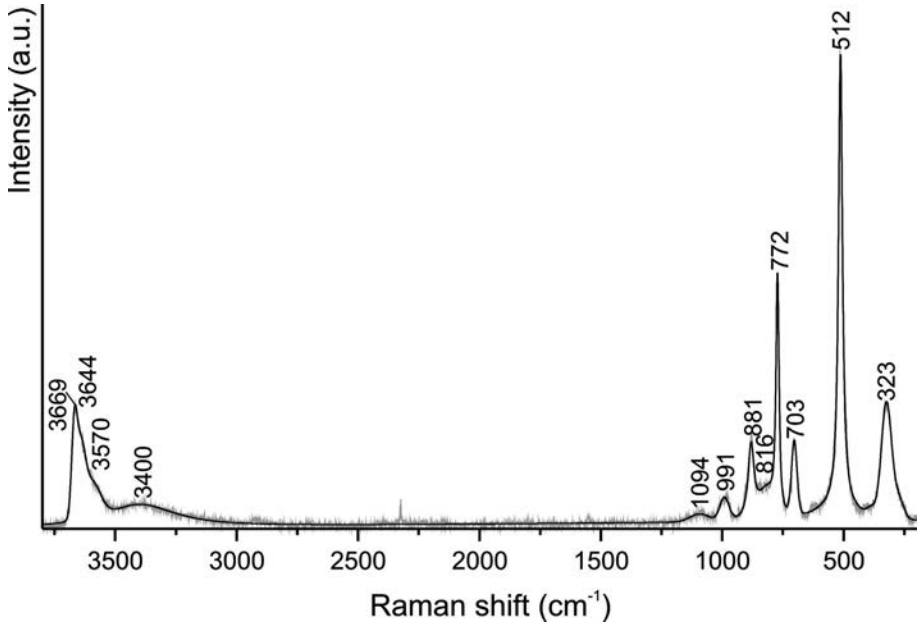

FIG. 3. The Raman spectrum of mayenite from the Eifel district.

probably connected with the hydration of a phase that initially had a composition corresponding to brearleyite, $Ca_{12}Al_{14}O_{32}Cl_2$ (Ma *et al*., 2011). Our single-crystal X-ray investigations show that there is partial substitution of O2 by 3 × O2a, which causes a change in Al coordination from tetrahedral to octahedral. This phenomenon is related to the partial hydration of $Ca_{12}Al_{14}O_{32}Cl_2$ according to the scheme $(O^{2-} + Cl^{-}) \leftrightarrow 3(OH)^{-}$. The formula for mayenite from the Eifel district can be written $Ca_{12}Al_{14}O_{32-x}Cl_{2-x}(OH)_{3x}$ (x ~0.75). The $Ca_{12}Al_{14}O_{32}Cl_2$ endmember is dominant (62.5 mol.%). However, this endmember has a composition that is different from the formula originally given for mayenite, $Ca_{12}Al_{14}O_{33}$. The $Ca_{12}Al_{14}O_{30}(OH)_6$ endmember is subordinate at 37.5 mol.%. A maximum of only 25% of O2 (x = 2) may be substituted in $Ca_{12}Al_{14}O_{32}Cl_2$ leading to the crystal chemical formula $Ca_{12}Al_{14}O_{30}(OH)_6$.

Our investigation of mayenite produces questions about the nature of the closely related mineral brearleyite. Ma *et al*. (2011) determined a = 11.98(8) Å for brearleyite, which is similar to a = 12.03204(3) Å for the Cl-rich hydrated mayenite studied here (Table 2). We cannot rule out the possibility that there are natural anhydrous halogen-bearing mayenite-like phases with compositions $Ca_{12}Al_{14}O_{32}Cl_2$ or $Ca_{12}Al_{14}O_{32}F_2$ (which might be preserved as inclusions). However, brearleyite occurs as porous aggregates with grain sizes of less than 1−2 μm, which make both EMPA and Raman investigations problematic. Further studies are required to prove its 'anhydrous' nature. The extremely high reactivity of mayenite has been confirmed experimentally (Park, 1998; Strandbakke *et al*., 2009). Ma *et al*. (2011) concluded that brearleyite does not contain OH groups on the basis of its Raman spectrum, which had very few absorption bands, such as the band near 320 cm^{-1}, the intensity of which is comparable with the intensity of the band from OH groups in our spectra of mayenite (Fig. 3). Thus, it is possible that OH was below the detection limit of Raman spectroscopy in the conditions which Ma *et al*. (2011) used to collect their spectrum.

The hydration of mayenite is commonly described by the reaction $Ca_{12}Al_{14}O_{32}O + H_2O \rightarrow Ca_{12}Al_{14}O_{32}(OH)_2$ (Ruszak *et al*., 2007; Strandbakke *et al*., 2009). Our data indicate that the capacity of the mayenite structure for OH groups may be even greater, following the equation $Ca_{12}Al_{14}O_{32}O + 3H_2O \rightarrow Ca_{12}Al_{14}O_{30}(OH)_6$. For this to occur, two Al cations p.f.u. must change their coordination from tetrahedral to octahedral (4 to 6). This type of reaction may be a first step (intermediate phase)

towards complete hydration, which would produce the garnet-group mineral katoite, $Ca_3Al_2(OH)_{12}$, a phase which is found in mayenite cement (Schröpfer and Bartl, 1993). If we further assume that this intermediate phase could inherit morphological features of the protocrystal, unusually large grossular–katoite pseudomorphs after a mayenite- or wadalite-like mineral might be expected. Such pseudomorphs have been described from the Wiluy River, Siberia, Russia under the name 'achtarandite' (Galuskin *et al*., 1995; Galuskina *et al*., 1998).

Acknowledgements

The authors thank Edward Grew for comments on the first draft version of the manuscript. The authors also thank R. James Evans and the anonymous reviewers for the careful revision that improved the early version of the manuscript. The work was partly supported by the Ministry of Science and Higher Education of Poland, grants no. N307 075239 (to E.V. and R.B.)

References

Bartl, H. and Scheller, T. (1970) Zur Struktur des $12CaO{\cdot}7A1_2O_3$. *Neues Jahrbuch für Mineralogie, Monatshefte*, **1970**, 547–552.

Boysen, H., Lerch, M., Stys, A. and Senyshyn, A. (2007) Structure and oxygen mobility in mayenite ($Ca_{12}Al_{14}O_{33}$): a high-temperature neutron powder diffraction study. *Acta Crystallographica*, **B63**, 675–682.

Boysen, H., Kaiser-Bischoff, I., Lerch, M., Berendts, S., Börger, A., Trots, D.M., Hoelze, M. and Senyshyn, A. (2009) Structures and properties of variously doped mayenite investigated by neutron and synchrotron powder diffraction. *Zeitschrift für Kristallographie*, *Supplement*, **30**, 323–328.

Boysen, H., Kaiser-Bischoff, I., Lerch, M., Berendt, S., Hoelzel, M. and Senyshyn, A. (2010) Disorder and diffusion in mayenite. *Acta Physica Polonica*, **117**, 38–41.

Büssem, W. and Eitel, A. (1936) Die Struktur des Pentacalciumtrialuminats. *Zeitschrift für Kristallographie*, **95**, 175–188.

Feng, Q. L., Glasser, F. P., Howie, R. A. and Lachowski, E. E. (1988) Chlorosilicate with the $12CaO{\cdot}7Al_2O_3$ structure and its relationship to garnet. *Supplement to Acta Crystallographica*, **C44**, 589–592.

Fujita, S., Suzuki, K., Ohkawa, M., Shibasaki, Y. and Mori, T. (2001) Reaction of hydrogrossular with hydrogen chloride gas at high temperature. *Chemistry of Materials*, **13**, 2523–2527.

Galuskin, E., Galuskina, I. and Winiarska, A. (1995) Epitaxy of achtarandite on grossular – the key to the problem of achtarandite. *Neues Jahrbuch für Mineralogie, Monatshefte*, **1995**, 306–320.

Galuskin, E.V., Gazeev, V.M., Lazic, B., Armbruster, T., Galuskina, I.O., Zadov, A.E., Pertsev, N.N., Wrzalik, R., Dzierzanowski, P., Gurbanov, A.G. and Bzowska, G. (2009) Chegemite – $Ca_7(SiO_4)_3(OH)_2$ – a new humite-group calcium mineral from the Northern Caucasus, Kabardino-Balkaria, Russia. *European Journal of Mineralogy*, **21**, 1045–1059.

Galuskin, E.V., Bailau, R., Galuskina, I.O., Prusik, A.K., Gazeev, V.M., Zadov, A.E., Pertsev, N.N., Jeżak, L., Gurbanov, A.G. and Dubrovinsky, L. (2011) Eltyubyuite, IMA 2011–022. CNMNC, Newsletter No. 10, October 2011, page 2553; *Mineralogical Magazine*, **75**, 2549–2561.

Galuskina, I., Galuskin, E. and Sitarz, M. (1998) Atoll hydrogarnet and mechanism of the formation of achtarandite pseudomorphs. *Neues Jahrbuch für Mineralogie*, *Monatshefte*, **1998**, 49–62.

Gross, S. (1977) The mineralogy of the Hatrurim Formation, Israel. *Geological Survey Israel Bulletin*, **70**, 10–11.

Hayashi, K. (2011) Kinetics of electron decay in hydride ion-doped mayenite. *Journal of the Physical Chemistry*, **115**, 11003–11009

Hentschel, G. (1964) Mayenit, $12CaO{\cdot}7Al_2O_3$, und Brownmillerit, $2CaO{\cdot}(Al,Fe)_2O_3$, zwei neue Minerale in den Kalksteineinschlüssen der Lava des Ettringer Bellerberges. *Neues Jahrbuch für Mineralogie*, *Monatshefte*, **1964**, 22–29.

Hosono, H., Hayashi, K. and Hirano, M. (2007) Active anion manipulation for emergence of active functions in the nanoporous crystal $12CaO{\cdot}7Al_2O_3$: a case study of abundant element strategy. *Journal of Material Sciences*, **42**, 1872–1883.

Hosono, H., Hayashi, K., Kajihara, K., Sushko, P.V. and Shluger, A.L. (2009) Oxygen ion conduction in $12CaO{\cdot}7Al_2O_3$: O^{2-} conduction mechanism and possibility of O^- fast conduction. *Solid State Ionics*, **180**, 550–555.

Iwata, T., Masahide, M. and Fukuda, K. (2008) Crystal structure of $Ca_{12}Al_{14}O_{32}Cl_2$ and luminescence properties of $Ca_{12}Al_{14}O_{32}Cl_2$: Eu^{2+}. *Journal of Solid State Chemistry*, **181**, 51–55.

Janek, J. and Lee, D.-K. (2010) Defect chemistry of the mixed conducting cage compound $Ca_{12}Al_{14}O_{33}$. *Journal of the Korean Ceramic Society*, **47**, 99–105.

Li, C., Hirabayashi, D. and Suzuki, K. (2009) A crucial role of O_2^- and O_2^{2-} on mayenite structure for biomass tar steam reforming over $Ni/Ca_{12}Al_{14}O_{33}$. *Applied Catalysis B: Environmental*, **88**, 351–360.

Ma, C., Connolly H.C. Jr, Beckett, J.R., Tschauner, O., Rossman, G.R., Kampf, A.R., Zega, T.J., Sweeney Smith, S.A. and Devin L. Schrader, D.L. (2011)

Brearleyite, $Ca_{12}Al_{14}O_{32}Cl_2$, a new alteration mineral from the NWA 1934 meteorite. *American Mineralogist*, **96**, 1199–1206.

Matsuishi, S., Toda, Y., Miyakawa, M., Hayashi, K., Kamiya, K., Hirano, M., Tanaka, I. and Hosono, H. (2003) High-density electron anions in a nanoporous single crystal: $[Ca_{24}Al_{28}O_{64}]^{4+}(4e^-)$. *Science*, **301**, 626–629.

Matsuishi, S., Nomura, T., Hirano, M., Kodama, K., Shamoto, S. and Hosono, H. (2009) Direct synthesis of powdery inorganic electride $[Ca_{24}Al_{28}O_{64}]^{4+}(e^-)_4$ and determination of oxygen stoichiometry. *Chemistry of Materials*, **21**, 2589–2591.

Mihajlović, T., Lengauer, K.L., Ntaflos, T., Kolitsch, U. and Tillmanns, E. (2004) Two new minerals, rondorfite, $Ca_8Mg[SiO_4]_4Cl_2$, and almarudite, $K(\square,Na)_2(Mn,Fe,Mg)_2$ $(Be,Al)_3Si_{12}O_{30}]$, and a study of iron-rich wadalite, $Ca_{12}[(Al_8Si_4Fe_2)O_{32}]Cl_6$, from the Bellerberg (Bellberg) volcano, Eifel, Germany. *Neues Jahrbuch für Mineralogie, Abhandlungen*, **179**, 265–294.

Palacios, L., De La Torre, A.G., Bruque, S., García-Muñoz, J.L., García-Granda, S., Sheptyakov, D. and Aranda, M.A.G. (2007) Crystal structures and *in-situ* formation study of mayenite electrides. *Inorganic Chemistry*, **46**, 4167–4176.

Palacios, L., Cabeza, A., Bruque, S., García-Granda, S. and Aranda, M.A.G. (2008) Structure and electrons in mayenite electrides. *Inorganic Chemistry*, **47**, 2661–2667.

Park, C.-K. (1998) Characteristic and hydration of $Ca_{12-x}A_7{\cdot}(CaF_2)$ (x = 0 ~ 1.5) minerals. *Cement and Concrete Research*, **28**, 1357–1362.

Qijun, Y., Sugita, S., Xiuju, F. and Jinxiao, M. (1997) On the preparation of single crystal of $11CaO{\cdot}7Al_2O_3{\cdot}CaF_2$ and the confirmation of its structure. *Cement and Concrete Research*, **27**, 1439–1449.

Ruszak, M., Witkowski, S. and Sojka, Z. (2007) EPR and Raman investigations into anionic redox chemistry of nanoporous $12CaO{\cdot}7Al_2O_3$ interacting with O_2, H_2 and N_2O. *Research on Chemical Intermediates*, **33**, 689–703.

Sakakura, T., Tanaka, K., Takenaka, Y., Matsuishi, S., Hosono H. and Kishimoto, S. (2011) Determination of the local structure of a cage with an oxygen ion in $Ca_{12}Al_{14}O_{33}$. *Acta Crystallographica*, **B67**, 193–204.

Schröpfer, L. and Bartl, H. (1993) Oriented decomposition and reconstruction of hydrogarnet, $Ca_3Al_2(OH)_{12}$. *European Journal of Mineralogy*, **5**, 1133–1144.

Sheldrick, G.M. (2008) A short history of *SHELX*. *Acta Crystallographica*, **A64**, 112–122.

Strandbakke, R., Kongshaug, C., Haugsrud, R. and Norby, T. (2009) High-temperature hydration and conductivity of mayenite, $Ca_{12}Al_{14}O_{33}$. *Journal of Physical Chemistry*, **C113**, 8938–8944.

Sun, J., Chong-fu Song, C., Ninga, S., Lina, S. and Lia, Q. (2009) Preparation and characterization of storage and emission functional material of chlorine anion: $[Ca_{24}Al_{28}O_{64}]^{4+}{\cdot}(Cl^-)_{3.80}(O^{2-})_{0.10}$. *Chinese Journal of Chemical Physics*, **22**, 417–422.

Tolkacheva, A.S., Shkerin, S.N., Plaksin, S.V., Vovkotrub, E.G., Bulanin, K.M., Kochedykova, V.A., Ordinartseva, D.P., Gyrdasova, O.I. and Molchanova, N.G. (2011) Synthesis of dense ceramics of single-phase mayenite $(Ca_{12}Al_{14}O_{32})O$. *Russian Journal of Applied Chemistry*, **84**, 907–911.

Tsukimura, K., Kanazawa, Y., Aoki, M. and Bunno, M. (1993) Structure of wadalite, $Ca_6Al_5Si_2O_{16}Cl_3$. *Acta Crystallographica*, **C49**, 205–207.

Williams, P.P. (1973) Refinement of structure of $11CaO{\cdot}7Al_2O_3{\cdot}CaF_2$. *Acta Crystallographica*, **B29**, 1550–1551.